Cytometry PART A
Journal of the International Society for Advancement of Cytometry

MIFlowCyt

Analysis of the Advantages of Cis Reporters in Optimized FACS-Gal

Miguel Ángel Sánchez-Luengo,[1] Miguel Rovira,[2] Manuel Serrano,[2] Pablo Jose Fernandez-Marcos,[2,3]* Lola Martinez[1]*

[1]Flow Cytometry Unit, Biotechnology Programme, Spanish National Cancer Research Centre (CNIO), Madrid, E28029, Spain

[2]Tumor Suppression Group, Molecular Oncology Programme, Spanish National Cancer Research Centre (CNIO), Madrid, E28029, Spain

[3]Bioactive Products and Metabolic Syndrome (BIOPROMET), Madrid Institute for Advanced Studies (IMDEA) in Food, CEI UAM + CSIC, Madrid, E28049, Spain

Received 11 October 2016; Revised 29 December 2016; Accepted 23 February 2017

Grant sponsor: Spanish Ministry of Economy and Competitiveness, Grant numbers: SEV-2011-0191; SEV-2015-0510

Additional Supporting Information may be found in the online version of this article.

*Correspondence to: Lola Martinez, Flow Cytometry Unit, Biotechnology Programme, Spanish National Cancer Research Centre (CNIO), Madrid E28029 Spain. E-mail: lmartinez@cnio.es
and
Pablo Jose Fernandez-Marcos, Tumor Suppression Group, Molecular Oncology Programme, Spanish National Cancer Research Centre (CNIO), Madrid E28029 Spain. E-mail: pablojose.fernandez@imdea.org

Published online 4 April 2017 in Wiley Online Library (wileyonlinelibrary.com)

DOI: 10.1002/cyto.a.23086

ISAC
International Society for Advancement of Cytometry

Abstract

Flow cytometry is a powerful multiparametric technology, widely used for the identification, quantification, and isolation of defined populations of cells based on the expression of target proteins. It also allows for the use of surrogate reporters, either enzymatic or fluorescent, to indirectly monitor the expression of these target proteins. In this work, we optimised the dissociation protocol for the detection of the enzymatic reporter *LacZ* using the FACS-Gal detection system with the fluorogenic substrate FDG to compare cis- versus trans-positioned reporters efficiency. Particularly, for the FACS-Gal optimization, we studied lung and haematopoietic tissues, focusing on cell recovery, viability, FDG loading conditions and distribution of cellular populations. Reporter genes such as *LacZ* can be placed together with the gene of interest in the same polycistronic mRNA (in cis), or in independent alleles (in trans), which can strongly affect the correlation with the reporter readout. To address this issue, we generated a mouse model containing both types of reporters for the same gene, and compared them. Our results clearly indicate that trans-positioned reporters can be misleading, and that using a reporter gene in cis rather than trans is a much more specific method to sort for cells undergoing Cre-mediated recombination. © 2017 International Society for Advancement of Cytometry

Key terms

FACS-Gal; LacZ; tissue dissociation; flow cytometry; Katushka; cis reporter; trans reporter

Introduction

An Overview on FACS-Gal System

Reporter genes are commonly used to study gene expression. This technology initially relied on the use of fusion genes encoding hybrid proteins, such as the *Escherichia coli* gene *LacZ* encoding β-galactosidase. *LacZ* has been one of the most common reporter genes since it was first used for gene expression analysis in *Caenorhabditis elegans* (1). Later on, reporter gene technology was enhanced with the discovery and cloning of the Green Fluorescent Protein (GFP) from *Aequorea victoria*. GFP can be directly measured, allowing the study of molecular localization in living cells (2). Since then, a number of GFP genetic variants were developed, and other reporters such as the Red Fluorescent Protein (RFP) were isolated. Reporter genes are routinely used in flow cytometry, and currently there is a large variety of fluorescent proteins with different spectral profiles and properties (3–5).

Fluorescent proteins have a widespread compatibility in tissues and organisms, allowing their use in the study of static and dynamic patterns in live animals. However, LacZ is still a very useful readout of gene expression, as β-galactosidase histochemistry affords sensitive, high-resolution protein localization (6). Moreover, β-galactosidase technology has also been adapted to flow cytometry, a powerful multiparametric and sensitive technology, with the FACS-Gal detection system (7). This

system is based on a fluorogenic substrate of the LacZ enzyme, fluorescein di-β-D-galactopyranoside (FDG), and it allows for the staining, analysis and flow-sorting of live cells according to their levels of *LacZ* expression. The detection assay is based on the loading of FDG into the cytoplasm, which is then hydrolyzed by β-galactosidases and retained inside the cell. Hydrolysis rate and therefore fluorescence intensity is proportional to the cellular concentration of the β-galactosidase reporter enzyme. However, LacZ detection by FACS-Gal is sensitive to the cell type, the fluorescent substrate, and the substrate loading conditions. Also, the isolation of cells for FDG staining from different tissues involves the use of mechanical and/or enzymatic dissociation methods. In general, mechanical disruption tends to be less efficient and more damaging to the cells than enzymatic digestion. However, enzymatic digestion may produce alterations in the cell membrane, affecting FDG loading efficiency as well as surface marker receptors. This is why the ability to sort LacZ+ and LacZ− cells with the FACS-Gal detection system remains a challenge.

Cis and Trans Inducible Reporter Models

Inducible genetic systems allow for conditional genetic modifications of gene expression and are widely used. Cre-ERT2 is a very common inducible system, consisting on the fusion of Cre recombinase with the DNA binding site of the estrogen receptor. Cre proteins recognize specific genetic sequences known as LoxP sites. These sites can be genetically designed to flank a sequence of interest, which will be excised upon Cre activation. The Cre-ERT2 chimeric protein stays inactive in the cytosol until it binds to estrogen or an analogue molecule, such as 4-hydroxy-tamoxifen (4-OHT). When this binding occurs, Cre-ERT2 translocates to the nucleus, and the Cre recombinase recognizes and recombines LoxP-flanked regions, excising and eliminating the intermediate sequence (8).

Some inducible gene activation systems consist on the insertion of a LoxP-flanked STOP cassette (LSL cassette) in the 5′ region of a gene of interest. This prevents the gene expression until the Cre recombinase excises the STOP cassette. Activation of the gene of interest can be monitored either by direct mRNA or protein quantification, or by reporter genes. Using an Internal Ribosome Entry Site (IRES), reporter genes can be placed together with the gene of interest in the same polycistronic mRNA (in cis), thus sharing the same regulatory sequences. Alternatively, genes of interest and reporter genes can be placed in independent alleles (in trans) and activated with the same mechanism, for example, with a LSL cassette preceding both alleles. Theoretically, the two alleles in trans would be activated with the same efficiency, although in practice the Cre recombination efficiency may differ between the two alleles.

In this article we evaluated the advantages of using the FACS-Gal detection system to study gene expression, focusing on two aspects: first, we studied FDG loading efficiency in different tissues (hematopoietic and non-hematopoietic), homogenized and processed by different methods involving or not the use of enzymes; secondly, we used the optimized FACS-Gal detection system, combined with a Katushka Red Fluorescent Protein (KFP) reporter, to compare the efficiency and sensitivity of cis- and trans-positioned reporters in the lung.

Materials and Methods

Animal Procedures

Wild type C57BL/6J and B6.129S4-Gt (ROSA) 26Sor^{tm1Sor}/J (with ubiquitous expression of LacZ) (9) were bred at the CNIO facilities. Transgenic mice *K-Ras*^{LSLG12Vgeo}, *Polr2a-Cre-ERT2*, and *CAG-KFP*^{LSL} were previously described (10,11). All animal procedures were approved by the CNIO-ISCIII Ethics Committee for Research and Animal Welfare (CEIyBA) and conducted in accordance with the recommendations of the Federation of European Laboratory Animal Science Associations (FELASA).

Cre-ERT2-mediated recombination was induced in 8- to 10-week-old mice by a diet supplemented with tamoxifen for 4 weeks (tamoxifen is metabolized in the liver into its active, Cre-ERT2-activating form 4-OHT), prior to fluorescence-activated cell sorting, to isolate the LacZ and/or KFP-expressing cells.

Tissue Preparation and Assessment of β-Galactosidase Activity

For mechanical disaggregation, bone marrow was flushed with RPMI medium supplemented with 10% fetal calf serum (FCS) from femurs and tibiae; thymus and spleen were cut into small pieces and disaggregated by grinding the tissues on a 40 μm cell strainer, and red blood cells were lysed with ammonium chloride for 10 minutes at 37°C (Qiagen, GmBH). For enzymatic digestion, hematopoietic tissues were processed as described below for the lungs, with the exception of the perfusion step.

Mouse lungs were intracardially perfused with 20 mL ice-cold PBS, then lungs were removed and 2 mL of 5 U/mL dispase (Corning, NY, USA) were injected intratracheally. Lungs were placed in a tube containing HBSS + 1% FBS. After 15 minutes of incubation with dispase at room temperature, digested lungs were cut into small pieces and transferred to a GentleMacs tube containing 7 mL HBSS, 1% FBS, 20 U/mL DNase I (Promega, WI, USA), and 70 U/mL collagenase I (Gibco, CA, USA). Then, samples were homogenized using the "mouse lung 1" GentleMacs program (Miltenyi, GmBH), incubated for 30 minutes at 37°C under shaking and homogenized again with the "mouse lung 2" GentleMacs program. The homogenized mixture was then filtered through a 70 μm cell strainer (BD, San Jose, CA) and centrifuged at 300*g* for 5 minutes. Supernatant was discarded and cell pellet was resuspended in 5 mL Quiagen lysis buffer for 10 minutes at 37°C for red blood cell lysis. Cells were then resuspended in RPMI + 10% FBS.

For mechanical disaggregation, lungs were intracardially perfused with 20 mL ice-cold PBS, removed and placed in a tube containing HBSS + 1% FBS. Then samples were homogenized in a GentleMacs as previously described, except this time using HBSS + 1% FBS, so that lungs were never in contact with any enzyme.

Cell counting and viability were evaluated using trypan blue (Sigma, GmBH) in an automated cell counter Countess (Molecular Probes, OR), and resuspended at 10^7 cells/mL in HBSS + 2% FBS containing 10 mM HEPES buffer (Gibco, CA, USA).

β-galactosidase activity was assessed according to Fiering et al. (12), using the fluorescein di-β-D-galactopyranoside (FDG, Thermo Fisher Scientific, Waltham, MA) vital substrate and following the protocol of Guo et al. (13). For FDG loading, 100 µL of cell suspension were aliquoted into pre-warmed FACS tubes containing 100 µL of 2 mM FDG solution in distilled water. Cell suspension was mixed and incubated at 37°C in a water bath for the indicated times. FDG uptake was stopped with 2 mL ice-cold HBSS + 2% FBS + 10 mM HEPES buffer. Cells were then centrifuged at 300*g* for 5 minutes, supernatant was discarded and cell pellet resuspended in 300 µL HBSS buffer.

For negative controls, the competitive inhibitor of β-galactosidase activity, phenylethyl β-D-thiogalactopyranoside (PETG, Thermo Fisher Scientific, MA), was added prior to the FDG loading to a final concentration of 1 mM.

Flow Cytometry

Following FDG loading, additional immunophenotyping was performed: hematopoietic samples were stained with either anti-B220 PE (dilution 1/200, BD, San Jose), anti-CD11b PE-Cy7 (dilution 1/200, BD, San Jose), and anti-CD45 APC (dilution 1/200, BD, San Jose) monoclonal conjugated antibodies; lung samples were stained with anti-CD31 PE (dilution 1/400, BD, San Jose) and anti-CD45 APC (dilution 1/200, BD, San Jose) monoclonal conjugated antibodies. 4′,6-Diamidino-2-Phenylindole, Dihydrochloride (DAPI) (Sigma, GmBH) was added for live/dead discrimination to a final concentration of 20 ng/mL and samples were immediately acquired in an LSR Fortessa or an InFlux (BD, San Jose). We used single compensation controls in beads (OneComp Beads, eBioscience) to assess and compensate for spectral overlapping, except for the Katuskha control where cells were used. Population gating was performed using fluorescence minus one controls (FMOs). To assess *K-Ras*^{LSLG12Vgeo} recombination levels, pneumocytes were isolated as CD31-CD45-FDG± KFP± in an InFlux high-speed cell sorter. For the viability assays performed with DAPI, we used a combined gating strategy of pulse processing, DAPI and scatter to exclude cell aggregates and cellular debris. Both instruments, our LSR Fortessa and InFlux are equipped with a 355, 488, 561, and 640 nm laser lines (BD, San Jose). At least 10.000 live single target events were collected and all data were analyzed using FlowJo v10.1 (Treestar, OR).

Quantitative PCR Primer Design

Specific quantitative PCR (qPCR) primers were designed to quantitatively analyze the rate of Cre-mediated recombination of the LoxP-flanked STOP cassette (LSL) in the *K-Ras*^{LSLG12Vgeo} allele. The primer set "genomic-DNA" was designed to quantify the number of chromosomal copies in each DNA sample. This value was used to normalize all subsequent qPCR values.

Table 1. qPCR primers

Genomic DNA Fwd	GCATACACGAGGCTGTCAGA
Genomic DNA Rvs	GTGCGGCTGTACCTATGGAT
K-Ras^{LSLG12Vgeo}-recombined Fwd	GCAATGGCCAGTACTAGTGAA
K-Ras^{LSLG12Vgeo}-recombined Rvs	CCGCACGTCTAAGAAACCAT

To determine the rate of recombination, the "*K-Ras*^{LSLG12Vgeo}-recombined" pair of primers was designed to anneal specifically to sequences at either side of the LSL sequence of the *K-Ras*^{LSLG12Vgeo} allele. These sequences are part of the construct used to generate the *K-Ras*^{LSLG12Vgeo} allele, and are not present in the *K-Ras* wild type allele. Without Cre-mediated excision, these primers will not generate any amplicon, as they anneal to fragments approximately 3.5 kb apart (corresponding to the LSL sequence). When Cre-mediated recombination takes place, the LSL sequence becomes excised and this primer set amplifies a 180 bp segment (Supporting Information Fig. 1). The efficiency of the recombination was calculated using the formula: $2^{[(\text{genomic-DNA CT})-(\text{K-Ras}LSLG12Vgeo\text{ CT})]}$. Please note that only one of the two K-Ras alleles harbors the knock-in *K-Ras*^{LSLG12Vgeo}, while there are two copies per genome of the genomic-DNA used as a reference. Therefore, an efficiency of recombination of 0.5 is considered as 100%.

Determination of LoxP-STOP-LoxP Recombination

Genomic DNA was extracted from FACS-sorted lung cells by cell lysis using Proteinase K/PCR Lysis Buffer [10 mM Tris pH8.5, 50 mM KCl, 1.5 mM $MgCl_2$, 0.01% gelatine (Sigma), 0.45% NP-40 (Sigma), 0.45% Tween 20 (Sigma)], supplemented with 500 µg/mL Proteinase K (Roche). Cells in PK lysis buffer were heated at 55°C for 30 minutes in agitation. Proteinase K was then inactivated at 95°C for 20 minutes. DNA concentration was measured by Qubit Fluorometric Quantitation prior to qPCR analysis.

For qPCR, equal amounts of each DNA sample were assayed in triplicate reactions in optical-grade 386-well plates (Applied Biosystems, Foster City, CA). Each reaction contained 5 µL of 2× SybrGreen (Applied Biosystems), 1 µL of DNA template, 3 µL of DNAse-free water, and 1 µL of 10 µM primer mix. All PCR runs were performed on a QuantStudio™ 6 Flex Real-Time PCR System using QuantStudio 6 and 7 Flex Real-Time PCR software v1.0 (Applied Biosystems). Reaction conditions were as follows: 10 minutes at 94°C followed by 40 cycles of 30 seconds at 94°C, 30 seconds at 60°C, and 30 seconds at 72°C (Table 1).

Statistical Analysis

Data were statistically analyzed using either the unpaired two-tailed Student's *t* test or the one-way ANOVA and Tukey's multiple comparison test. Data were represented as the mean of the indicated experimental replicates. Error bars represent the standard error of the mean (s.e.m.). *, $P < 0.05$; **, $P < 0.01$; *** $P < 0.001$.

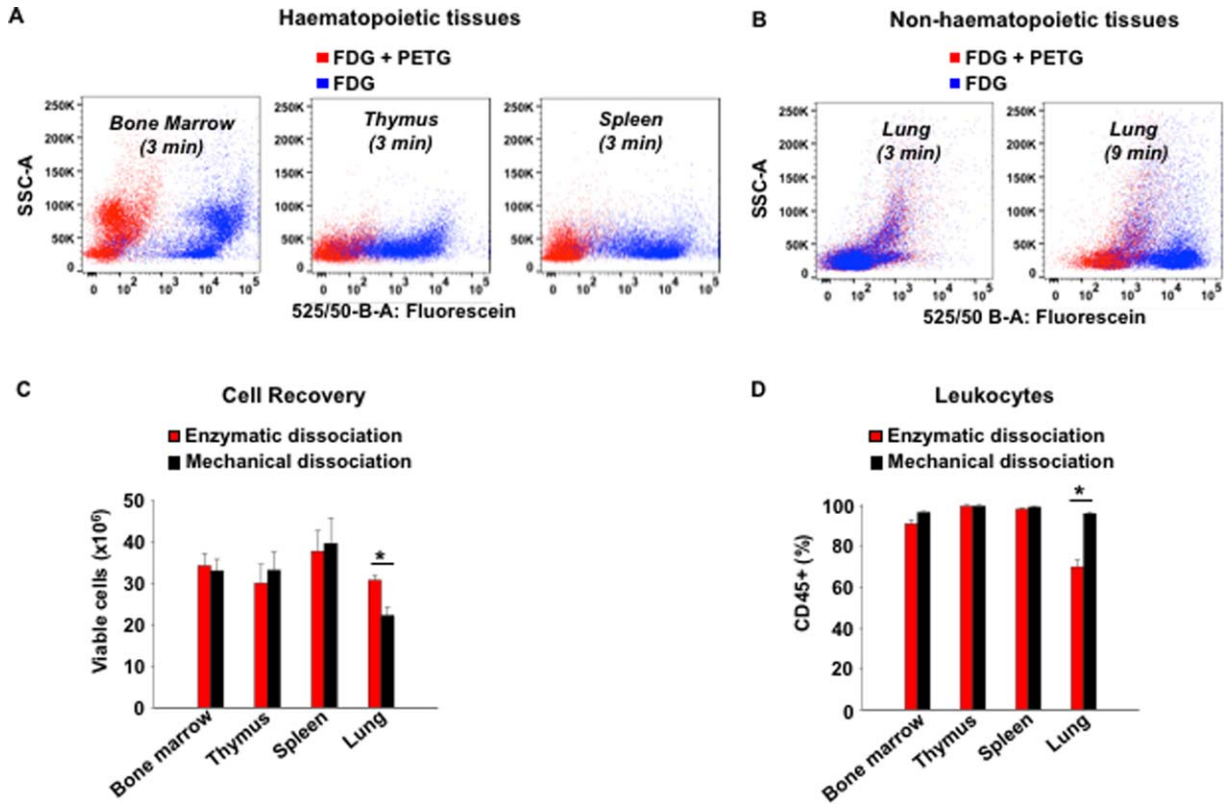

Figure 1. Comparison of FDG loading, cell recovery, and leucocyte count of the enzymatic versus mechanical dissociation protocols in hematopoietic tissues and lung. Fluorescein (blue) and background (red) signals were obtained after the indicated FDG loading time in hematopoietic tissues (A) and lung (B) from mice constitutively expressing LacZ. Background signal was defined by loading samples with the competitive inhibitor of β-galactosidase activity PETG prior to the FDG loading. (A) In all hematopoietic tissues, three minutes of hypotonic loading of FDG is enough to get a clear staining of the LacZ+ cells. (B) In the lung, loading time needs to be increased up to 9 minutes to obtain similar results. Hematopoietic tissues were processed mechanically, and lungs were processed enzymatically. Representative dot plots are shown. (C) Cell recovery was assessed on an automated cell counter (Countess, Invitrogen) using trypan blue to exclude dead cells from the counting. (D) Leukocyte fraction on live, DAPI-negative cells was identified as CD45+ cells. Bars represent the mean from six experiments. Error bars represent the standard error of the mean (s.e.m). Statistical significance was assessed using the unpaired two-tailed Student's *t test*. *: $P < 0.05$. [Color figure can be viewed at wileyonlinelibrary.com]

Results

Optimization of FACS-Gal Detection System in Lung and Hematopoietic Tissues

To use LacZ as an in vivo reporter, we performed FACS-Gal analysis on the B6.129S4-Gt (ROSA)26Sor*tm1Sor*/J mouse model, constitutively expressing LacZ. We focused on the lung and different hematopoietic tissues (bone marrow, spleen, and thymus). For flow cytometry analysis, hematopoietic tissues were isolated mechanically, while the lung was isolated enzymatically, and cells were loaded with the fluorogenic substrate FDG. Background signal was defined by treating cells with the FDG competitive inhibitor phenylethyl β-D-thiogalactopyranoside (PETG) prior to FDG loading. Previous reports indicate that 1–3 minutes of FDG loading time is enough to identify LacZ+ cells in hematopoietic tissues (12–16), which we confirmed (Fig. 1A). However, we observed that lung requires a longer loading time to detect FDG signal (Fig. 1B).

Thus, to optimize FACS-Gal detection protocol, we carried out a full comparison on the different isolation methods (either mechanical or enzymatic) to get good quality single-cell FDG-stained samples on the previously mentioned tissues. We focused on cell viability, cell recovery, and FDG loading conditions.

To study cell viability, total live cells were counted on a Countess automated cell counter using trypan blue to exclude dead cells. We did not observe major differences in the cell recovery of hematopoietic tissues, and only a slight decrease in the lung when processed mechanically compared with enzymatically (Fig. 1C). These same samples were stained with anti-mouse CD45 antibody and analyzed in a flow cytometer to assess the percentage of live leukocytes, identified as DAPI− and CD45+. No differences were observed in hematopoietic tissues in terms of percentage of leukocytes. However, there was a significant difference in the case of the lung, where we obtained over 20% more CD45+ cells when isolated with the mechanical protocol, compared with the enzymatic protocol (Fig. 1D). The higher percentage of leukocytes and the reduced cell viability in the lung indicate extensive death of pneumocytes, which may be due to pneumocytes not being

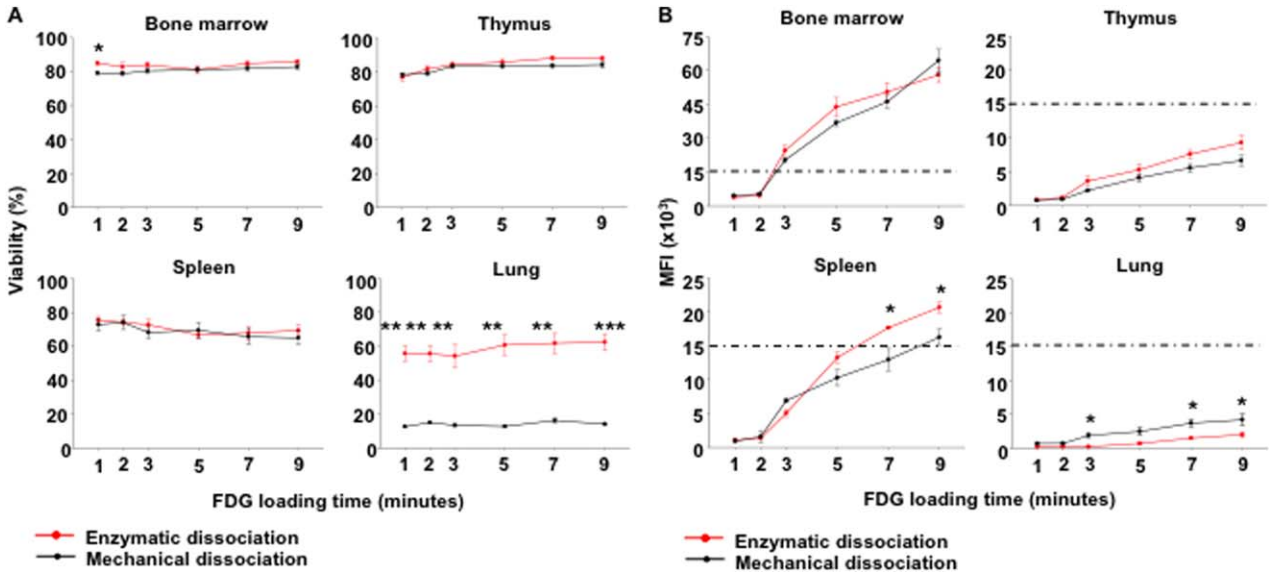

Figure 2. Survival rates and signal intensity upon FDG loading in hematopoietic and lung samples prepared using the enzymatic or mechanical dissociation protocols. (A) Graphs represent the cell viability of the indicated tissues using DAPI as a dead discriminator marker. Viability is affected by the processing protocol in the lung but not in the hematopoietic tissues. Dots represent the mean of six independent experiments. Error bars represent the standard error of the mean (s.e.m.). (B) FDG signal was evaluated by the median fluorescence intensity (MFI) of the FDG fluorescent product, fluorescein. Dots represent the mean of six experiments, and error bars represent the s.e.m. Statistical significance was assessed using the unpaired two-tailed Student's *t* test. *, $P<0.05$, **, $P<0.01$. [Color figure can be viewed at wileyonlinelibrary.com]

properly released from the extracellular matrix during mechanical processing. These results justify the widespread use of the enzymatic method for lung disaggregation.

To evaluate the possible effect of longer FDG loading times on cell survival, we performed a time course experiment for the hypotonic FDG loading into the different tissues. Viable cells were quantified by DAPI staining, using the gating strategy described in "Materials and Methods," to avoid including cellular debris on the viability quantification, and the median fluorescence intensity (MFI) of the fluorescent product (fluorescein) was quantified on the flow cytometer (Fig. 2). Survival rates were almost identical in all the studied hematopoietic tissues (bone marrow, thymus and spleen) (Fig. 2A). All of them presented at least 80% viability independently of the isolation method. As shown in Figure 2A, increasing FDG loading times did not affect cell viability in any tissue. Strikingly, viability was strongly decreased to less than 20% in lungs processed mechanically (Fig. 2A), indicating that, in lung, mechanical processing was more aggressive than the enzymatic protocol.

We continued optimizing FDG loading time, isolating single cell suspensions enzymatically or mechanically and loading them with either FDG (samples) or FDG plus the competitive inhibitor PETG (negative controls). A time course was performed for FDG loading under hypotonic conditions. For hematopoietic tissues shorter loading times are enough to resolve a positive population from the PETG-treated negative controls. In the case of the lung, as shown in Figure 1B, 9 minutes of loading time rendered a good resolution (Fig. 2B and Supporting Information Fig. 2).

Interestingly, FDG MFI signals were quite different in magnitude in the different tissues, being highest in the bone marrow, intermediate in the spleen and lowest in thymus and lung (Fig. 2B). Also, in lung there was higher MFI with the mechanical dissociation at the required FDG loading times to resolve LacZ-positive cells (7 and 9 minutes). We hypothesized that these divergences in MFI could be explained by the different distribution of populations within those tissues. In order to prove this, we compared the distribution of myeloid and B-cells in the different tissues according to the expression of CD11b (myeloid cells) and B220 (B-lymphocytes) processed mechanically or enzymatically. Hematopoietic samples were hypotonically loaded with FDG for 3 minutes, and lung samples were loaded with FDG for 9 minutes. Next, all samples were stained with an antibody cocktail containing PE-conjugated anti-mouse B220 and PE-Cy7-conjugated anti-mouse CD11b. Finally, DAPI was added and samples were immediately run on the flow cytometer.

We observed different population distributions in the hematopoietic tissues (Figs. 3A and 3B), with a higher percentage of myeloid cells in the bone marrow and of B-cells in spleen. In thymus, myeloid and B-cell populations are marginal, and T-cells (the most abundant cell type) fall into the "other cells" fraction. The MFI values in bone marrow for both myeloid and B cells are still higher compared with the same populations in the other tissues (Fig. 3C). These results indicate that the observations shown in Figure 2B (that FDG MFI is highest in bone marrow, intermediate in spleen and lowest in thymus), cannot be fully explained by the different cell distributions in each tissue.

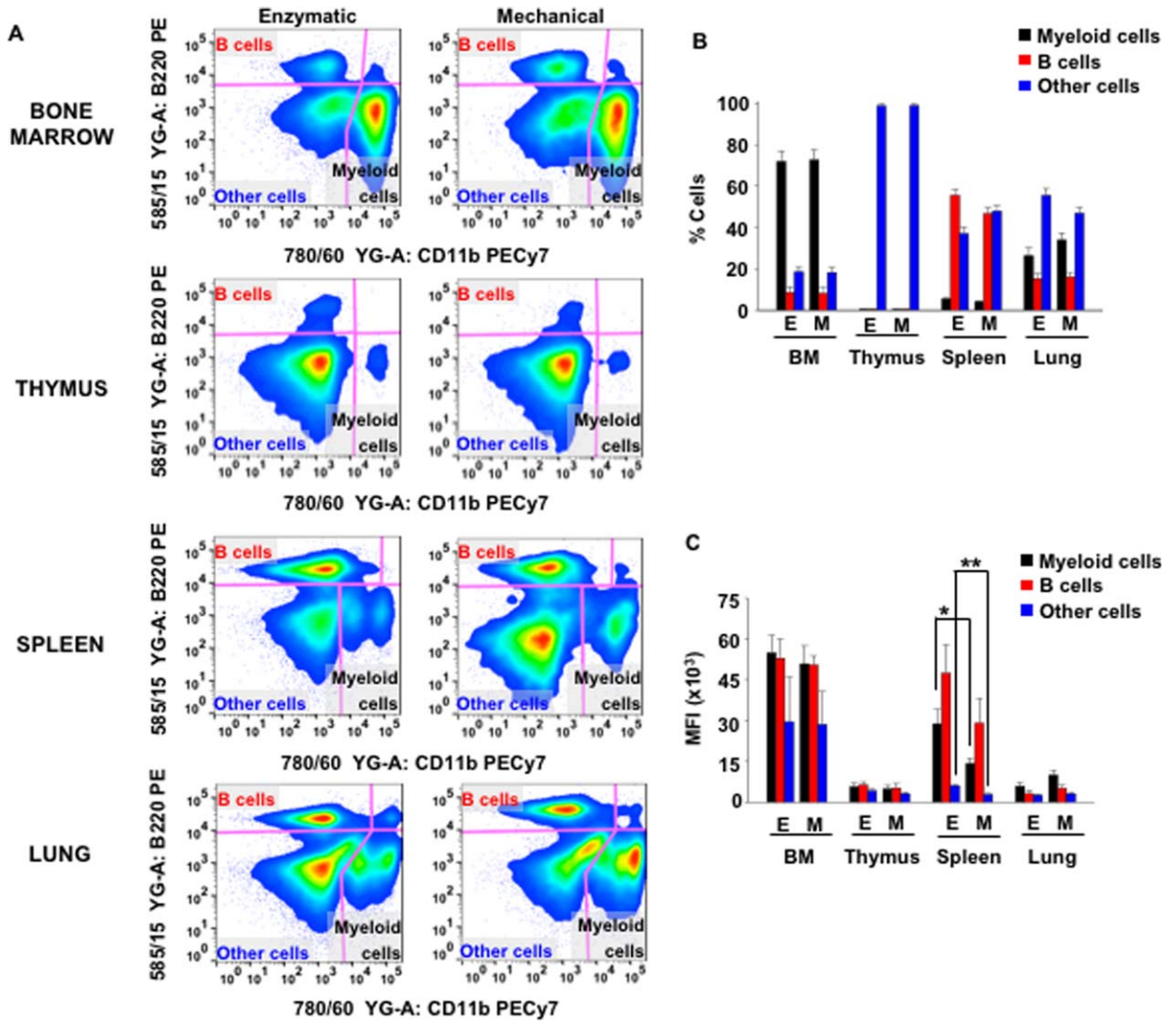

Figure 3. Cellular distribution and median fluorescence intensities of the FDG in the lung and hematopoietic tissues upon enzymatic or mechanical isolation. (A) Representative density plots of the distribution of myeloid (identified as CD11b+) and B cells (identified as B220+) in enzymatically or mechanically-processed lung and hematopoietic tissues. (B) Quantification of the cellular distribution of myeloid, B and other cells in lung and hematopoietic tissues processed enzymatically (E) or mechanically (M). In enzymatically processed lungs, the "other cells" fraction, containing the pneumocytes, shows a tendency to be increased. (C) MFI of the different cellular subsets in lung and hematopoietic tissues loaded with FDG for 9 minutes. As previously observed bone marrow MFI in all the subsets is higher than the same populations in spleen and thymus. Graphs represent the mean of three independent experiments and error bars represent the s.e.m. Statistical significance was assessed using the unpaired two-tailed Student's *t* test. *, $P<0.05$, **, $P<0.01$. [Color figure can be viewed at wileyonlinelibrary.com]

In lung, the CD11b B220 double negative fraction, which contained the pneumocytes (referred to as "other cells") tended to be higher in the enzymatically dissociated samples (Figs. 3A and 3B). We also observed that the myeloid fraction (CD11b+) showed a tendency for higher FDG MFI in the mechanically processed samples (Fig. 3C). Importantly, as suggested in Figure 1D, mechanically processed lung greatly increased the percentage of leukocytes (CD45+), and decreased the percentage of endothelial cells (CD31+) and pneumocytes (CD45−CD31−), compared with enzymatically processed samples, indicating that mechanical processing affects viability of non-leukocyte populations (Supporting Information Fig. 3). These observations could explain the higher MFI previously observed in the mechanically processed lungs (Fig. 2B).

All previous observations indicate that in the lung, mechanical isolation is less efficient and more damaging than enzymatic isolation, as shown in Figure 2A. This damage seems to affect mostly the pneumocyte-containing fraction, defined as CD45− in Figure 1D or CD11b−B220− in Figures 3A and 3B. Thus, we conclude that enzymatic dissociation is clearly the best method to isolate pneumocytes for further studies, in this case LacZ detection. In hematopoietic tissues no differences were observed between both isolation methods

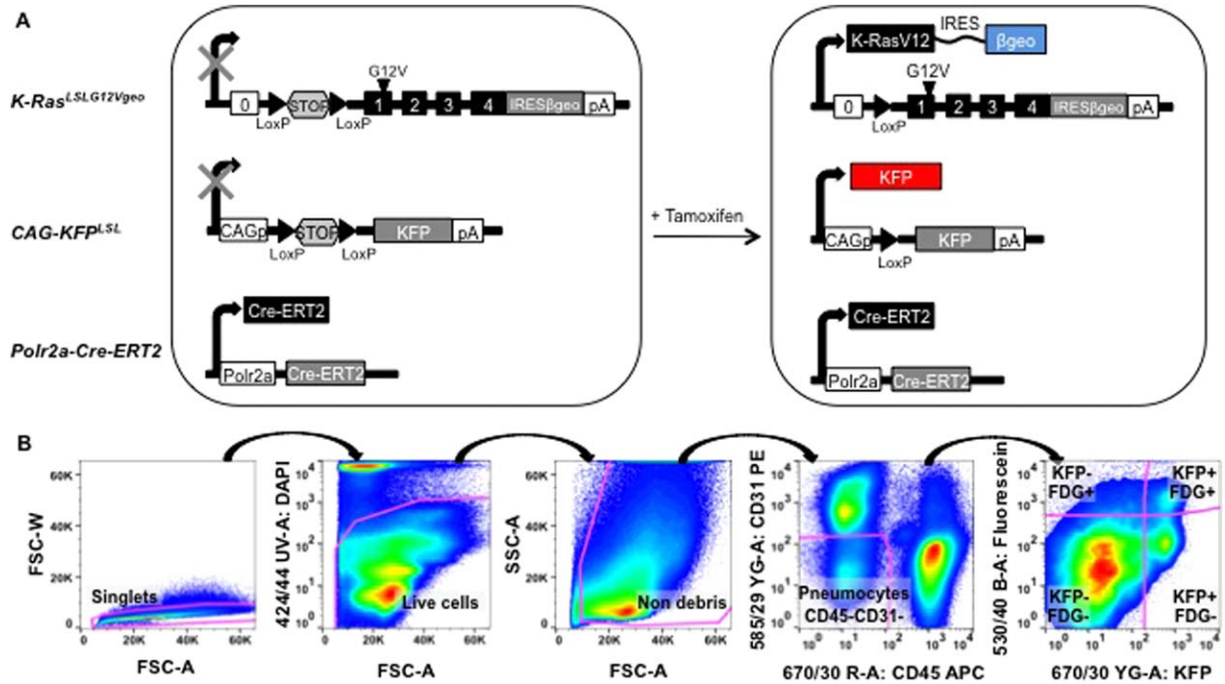

Figure 4. Isolation of pneumocytes from a mouse model presenting reporter genes in cis and trans with respect to the target gene. (A) Scheme depicting *K-Ras*^{LSLG12Vgeo}, *CAG-KFP*^{LSL}, and *Polr2a-Cre-ERT2* alleles and their mRNA products before and after tamoxifen-inducible, Cre-mediated recombination. 0: 5′ untranslated exon. LoxP: Cre-recombinase recognition sequence. STOP: transcription stop cassette. IRESβgeo: internal ribosome entry site followed by the *LacZ* gene. pA: poly-adenylation site. CAGp: CAG promoter. KFP: Katushka fluorescent protein. Polr2a: promoter of the RNA polymerase II subunit A. (B) Gating strategy used to identify the different subpopulations of pneumocytes based on their levels of KFP and/or FDG. Cells were sorted using pulse processing to exclude cell aggregates; DAPI was used as a dead discriminator; and CD45 and CD31 were used to exclude leukocytes (CD45+) and endothelial cells (CD31+) and select for the pneumocyte population. [Color figure can be viewed at wileyonlinelibrary.com]

either in terms of viability (Figs. 1C and 2A) or in terms of cellular distribution (Figs. 3A and 3B). Since the mechanical protocol is simpler and less time-consuming than the enzymatic one, we regard it as the best isolation method for hematopoietic tissues.

Comparison Between Reporter Genes in Cis Versus Trans

As explained before, reporters can be placed in the same polycistronic mRNA with the gene of interest using an IRES sequence (in cis) or placed in a different allele (in trans). To clarify the difference between these two reporter strategies, we crossed a mouse line harboring a Cre-ERT2-inducible KRas with a LacZ reporter in cis (*Polr2a-Cre-ERT2, K-Ras*^{LSLG12Vgeo}, from now on *K-Ras*^{G12VLSLgeo}) (10), with a mouse line harboring an inducible fluorescence Katushka (*CAG-KFP*^{LSL}, from now on KFP) in trans (11). Importantly, the *K-Ras*^{LSLG12Vgeo} allele is lethal in homozygosis (10), so both LacZ and KFP reporters were kept in heterozygosis to allow for a proper comparison between their signals. We induced Cre-ERT2-mediated recombination in these mice by tamoxifen diet administration, thus inducing the expression of the KFP and LacZ reporters (Fig. 4A). To assess the efficiency of excision of the gene of interest using each of the reporter genes, lungs from these mice were processed following the enzymatic protocol described in the materials and methods section. From the obtained single-cell pneumocyte suspension, 1 million cells were resuspended and loaded with FDG for 9 minutes. Immunophenotyping staining was then performed with APC-conjugated anti-mouse CD45 and PE-conjugated anti-mouse CD31 antibodies. DAPI was then added to samples to exclude dead cells and the populations of interest were identified following the gating strategy described in Figure 4B. Based on the expression of LacZ (FDG signal) and KFP, four subpopulations were defined, gated and sorted (Fig. 4B).

The fact that not all the cells expressing LacZ also express KFP (and vice-versa) indicated that the Cre-recombination efficiency differs between the LacZ cis reporter and the KFP trans reporter. To further analyze the Cre-recombination efficiency of the populations defined by the two different reporters, we isolated genomic DNA from the four subpopulations of pneumocytes (Fig. 4B), and quantified LSL recombination of the *K-Ras*^{G12VLSLgeo} allele by qPCR, using an independent genomic region as a reference for normalization. Since both *K-Ras*^{G12VLSLgeo} and KFP alleles were kept in heterozygosis, the theoretical optimum recombination efficiency with respect to the independent genomic control is 0.5, which we considered 100% (see Materials and Methods). In order to assess the efficiency of the different reporters (KFP or FDG), we took into account the percentage of cells in each of those four subpopulations (Figs. 5A and 5B), and normalized the *K-Ras*^{G12VLSLgeo} recombination efficiency to these percentages (Fig. 5C). Importantly, the KFP+FDG− cells, accounting for 84% of all

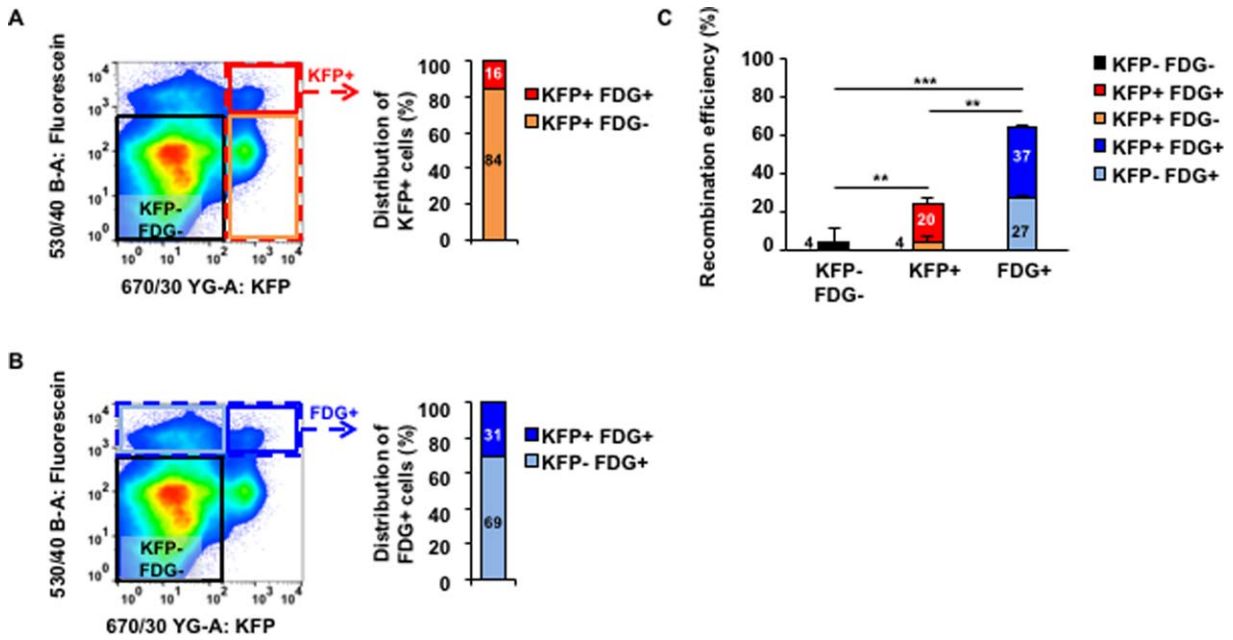

Figure 5. Evaluation of the recombination efficiency of the *K-Ras*^{LSLG12Vgeo} allele using reporters in cis or trans. (A) Distribution of pneumocyte populations from *K-Ras*^{LSLG12Vgeo}, *Polr2a-Cre-ERT2, CAG-KFP*^{LSL} mice according to their KFP expression (KFP+ FDG±) relative to all KFP positive cells. (B) Distribution of pneumocyte populations from *K-Ras*^{LSLG12Vgeo}, *Polr2a-Cre-ERT2, CAG-KFP*^{LSL} mice according to their FDG expression (KFP± FDG+) relative to all FDG positive cells. (C) Quantitative PCR of the recombined *K-Ras*^{LSLG12Vgeo} allele of genomic DNA from the sorted lung cells from each of the populations defined in the density plots in panels A and B, and normalized to the percentage of cells in each fraction (right bar graphs of panels A and B). There are significant differences regarding the recombination efficiency of *K-Ras*^{LSLG12Vgeo} allele, showing a high efficiency in the FDG+ fractions versus the KFP+. Bars represent the mean of five independent experiments. Error bars represent the s.e.m. Statistical significances were assessed using one-way ANOVA and Tukey's multiple comparison test. *, $P < 0.05$, **; $P < 0.01$; ***, $P < 0.001$. [Color figure can be viewed at wileyonlinelibrary.com]

KFP+ cells (Fig. 5A), contributed only 4% to the Cre recombination efficiency, similar to the KFP−FDG− population (Fig. 5C), while the KFP+FDG+ subpopulation, accounting for only 16% of all KFP+ cells (Fig. 5A), contributed five times more (20%) to the Cre recombination efficiency (Fig. 5C). In the case of the FDG cells (Fig. 5B), KFP−FDG+ cells (69% of all FDG+ cells) contributed 27% to the Cre recombination, and the KFP+ FDG+ cells (31% of all FDG+ cells) had a similar contribution (37%) to the Cre recombination efficiency (Fig. 5C).

Therefore, selecting for the trans KFP reporter, compared with the use of the cis FDG reporter, leads to the loss of many recombined cells (the KFP−FDG+ cells, false negatives), and the inclusion of many cells with no *K-Ras*^{G12VLSLgeo} recombination (the KFP+FDG− cells, false positives). These results show that using a reporter gene in cis rather than a reporter in trans is a much more specific method to flow-sort for cells undergoing Cre-mediated recombination, as the reporter in cis (FDG) rends fewer false negative and false positive events.

Discussion

In this work, we have optimized conditions for the in vivo detection of LacZ in mouse lungs and hematopoietic tissues by flow cytometry to compare the efficiency of cis and trans reporters. Classically the use of FACS-Gal detection system has been mainly restricted to hematopoietic samples, and in fact there is not much literature concerning its use in other cell types. In terms of FDG loading time, there is no consensus in the literature even for the hematopoietic tissues. It is clear from the work of Fiering et al. (12) that an increase in FDG loading time rendered higher FDG MFI. Similar data was also shown by Lorincz et al. (16), and in both cases 1 minute FDG loading was used. Other reports used longer FDG loading times, but never longer than 2 minutes (14,15). As we wanted to assess the optimal FDG loading time, we carried out a complete time course. In accordance with previous reports, we confirmed that 1 minute FDG loading was enough to resolve the LacZ-positive population. However, we observed better resolution at 3 minutes without compromising cell viability. Not surprisingly in the lung, longer FDG loading time was required to get good resolution for the FDG-positive cells compared with the negative controls. As our data shows, 9 minutes FDG loading allows for good MFI signals, without any impact on cell viability.

Our in-depth analysis in lung in terms of viability, FDG loading and cellular population distribution clearly shows that the enzymatic disaggregation should be the chosen protocol when the interest of the study is focused in the pneumocyte fraction. However, if the objective is to look at immune cells in the lung, as it is usually the case with hematopoietic tissues, the mechanical protocol should be considered, as it is simpler and less time-consuming than the enzymatic protocol.

In-vivo reporters are widely found in the literature. Fluorescent proteins are the most frequent choice, since they do not require any processing steps to detect them. Some studies in flies and bacteria comparing the sensitivity of fluorescent reporters and LacZ, concluded that both reporters are similar in terms of sensitivity (6,17). To our knowledge, there are no publications comparing either of those reporters positioned in cis or trans with respect to the gene of interest. In theory LoxP-flanked sequences should be recombined with the same efficiency by the Cre-recombinase. However, in practice this is often not the case, which can strongly affect the overall results. This is especially relevant since there are many mouse models where the fluorescent reporter is positioned in trans with the gene of interest. In our lung model, the LacZ reporter is positioned in cis with our gene of interest (*K-Ras*); and a red fluorescent protein, Katushka (*KFP*), positioned in trans. As our data indicates, the use of trans-positioned reporters as a direct readout of the gene of interest could be misleading: some recombined cells are not identified by the KFP reporter (KFP−FDG+, false negatives), and many non-recombined cells are included (KFP+FDG−, false positives). This could compromise the analysis and conclusions if such approach is used to flow-sort those cells for further characterization.

The efficiency of recombination never reached the theoretical optimum of 100% (that is, 0.5 of excised *K-Ras*^{G12VLSLgeo} or *KFP* alleles with respect to the independent genomic reference). Using the *K-Ras*^{G12VLSLgeo} reporter in cis, the efficiency was close to 64% (Fig. 5C), while the efficiency for the KFP was 24%. We understand that this difference with the theoretical optimum efficiency is due to technical issues, such as sorting of false positives, technical limitations with the qPCR, or others, and these issues will exist irrespective of the type of reporter being used. In any case, our results clearly show that using a cis-positioned reporter allows for an efficiency of recombination much closer to the theoretical optimum than using a trans-positioned reporter.

Altogether, our recommendation is to use preferentially cis-positioned reporters if available, since they are more specific than those positioned in trans with the gene of interest. If that option is not possible, the efficiency of excision of the target gene should be quantified to estimate possible sample contamination with non-recombined cells.

Acknowledgments

We thank R. Dieguez-Hurtado and S. Ortega for their Katuskha Cre-reporter transgenic mice. We are also thankful to the rest of the members of the flow cytometry unit, E. Garrido, T. López-Briones, and specially U.P. Cronin for critical reading and corrections of the manuscript. Work in L.M unit was funded by the CNIO. M.A.S-L was recipient of a contract from the Spanish Ministry of Economy and Competitiveness, grants SEV-2011-0191 and SEV-2015-0510, Centre of Excellence Severo-Ochoa. M.R. was supported by a "La Caixa"-Severo Ochoa PhD fellowship. P.J.F.M. was financed by the Spanish Association Against Cancer (AECC).

Literature Cited

1. Fire A, Harrison SW, Dixon D. A modular set of lacZ fusion vectors for studying gene expression in Caenorhabditis elegans. Gene 1990;93:189–198.
2. Chalfie M, Tu Y, Euskirchen G, Ward WW, Prasher DC. Green fluorescent protein as a marker for gene expression. Science 1994;263:802–805.
3. Heim R, Prasher DC, Tsien RY. Wavelength mutations and posttranslational autoxidation of green fluorescent protein. Proc Natl Acad Sci U S A 1994;91:12501–12504.
4. Heim R, Tsien RY. Engineering green fluorescent protein for improved brightness, longer wavelengths and fluorescence resonance energy transfer. Curr Biol 1996;6: 178–182.
5. Wachter RM, Elsliger MA, Kallio K, Hanson GT, Remington SJ. Structural basis of spectral shifts in the yellow-emission variants of green fluorescent protein. Structure 1998;6:1267–1277.
6. Timmons L, Becker J, Barthmaier P, Fyrberg C, Shearn A, Fyrberg E. Green fluorescent protein/beta-galactosidase double reporters for visualizing Drosophila gene expression patterns. Dev Genet 1997;20:338–347.
7. Nolan GP, Fiering S, Nicolas JF, Herzenberg LA. Fluorescence-activated cell analysis and sorting of viable mammalian cells based on beta-D-galactosidase activity after transduction of Escherichia coli lacZ. Proc Natl Acad Sci U S A 1988;85: 2603–2607.
8. Feil S, Valtcheva N, Feil R. Inducible Cre mice. Methods Mol Biol 2009;530:343–363.
9. Soriano P. Generalized lacZ expression with the ROSA26 Cre reporter strain. Nat Genet 1999;21:70–71.
10. Guerra C, Mijimolle N, Dhawahir A, Dubus P, Barradas M, Serrano M, Campuzano V, Barbacid M. Tumor induction by an endogenous K-ras oncogene is highly dependent on cellular context. Cancer Cell 2003;4:111–120.
11. Diéguez-Hurtado R, Martín J, Martínez-Corral I, Martínez MD, Megías D, Olmeda D, Ortega S. A Cre-reporter transgenic mouse expressing the far-red fluorescent protein Katushka. Genesis 2011;49:36–45.
12. Fiering SN, Roederer M, Nolan GP, Micklem DR, Parks DR, Herzenberg LA. Improved FACS-Gal: Flow cytometric analysis and sorting of viable eukaryotic cells expressing reporter gene constructs. Cytometry 1991;12:291–301.
13. Guo W, Wu H. Detection of LacZ expression by FACS-Gal analysis. Protoc. Exch 2008.
14. Elefanty AG, Begley CG, Metcalf D, Barnett L, Köntgen F, Robb L. Characterization of hematopoietic progenitor cells that expressthe transcription factor SCL, using a lacZ "knock-in" strategy. Proc Natl Acad Sci U S A 1998;95:11897.
15. Feuillard J, Mémet S, Goudeau B, Lilienbaum A, Schmidt-Ullrich R, Raphaël M, Israël A. In vivo identification of lymphocyte subsets exhibiting transcriptionally active NF-κB/Rel complexes. Int Immunol 2000;12:613–621.
16. Lorincz M, Roederer M. Reporters of gene expression: Enzymatic assays. Curr Protoc Cytom 2001;Chapter 9:Unit 9.5.
17. Garcia HG, Lee HJ, Boedicker JQ, Phillips R. Comparison and calibration of different reporters for quantitative analysis of gene expression. Biophys J 2011;101:535–544.